UMCM #1432813, VOL 0, ISS 0

Modeling of simultaneous shape memory and pseudoelastic effects of shape memory alloys on nonlinear dynamic response of multilayer composite plate embedded with pre-strained SMA wires under thermal condition

M. Botshekanan Dehkordi

QUERY SHEET

This page lists questions we have about your paper. The numbers displayed at left can be found in the text of the paper for reference. In addition, please review your paper as a whole for correctness.

Q1. Au: Please provide missing affiliation (Primary Institution, State).
Q2. Au: Please provide complete postal address.
Q3. Au: Please provide Figures in text citation for Figure 1, 9, and 10.
Q4. Au: Please note that Figure 3 is repeated twice. Please check and renumber Figures as well text citation, if needed.

TABLE OF CONTENTS LISTING

The table of contents for the journal will list your paper exactly as it appears below:

MECHANICS OF ADVANCED MATERIALS AND STRUCTURES
2018, VOL. 0, NO. 0, 1–12
https://doi.org/10.1080/15376494.2018.1432813

Taylor & Francis
Taylor & Francis Group

ORIGINAL ARTICLE

Check for updates

Modeling of simultaneous shape memory and pseudoelastic effects of shape memory alloys on nonlinear dynamic response of multilayer composite plate embedded with pre-strained SMA wires under thermal condition

M. Botshekanan Dehkordi

Q1 Shahrekord University, Faculty of Engineering, Shahrekord, Iran

ABSTRACT

Shape memory alloys as a kind of smart materials, have two unique characteristics entitled shape memory and pseudoelastic effects. In this paper, a nonlinear dynamic analysis of multilayered composite plate embedded with pre-strained SMA wires under thermal condition is implemented considering both effects of SMAs simultaneously, for the first time. The constitutive equation proposed by Brinson is used for modelling the behaviors of SMA wires. In this work, equations of motion are derived in the framework of Carrera's Unified Formulation, for robust analysis of the problem. In this regard, the nonlinear strains are employed for modelling the thermal effects and also the effect of recovery stresses in the SMA wires. In this study not only the material properties are instantaneous variable with respect to the time and location, but they are also unknown, which make the problem more complicated. For this aim, a transient nonlinear finite element in conjunction with incremental iterative algorithm proposed by the author is employed, in order to solve the equations. Results show that upon the thermal condition, the recovery stress is generated in the SMA wires and therefore reduce the amplitude of a damped response of the plate. One conclusion from this study is that, in contrast with many studies reported before, it cannot be always say that the stress recovery in SMA wires is increased with increasing the pre-strain of SMA wires. In other words, for a specified increasing in temperature, only a limit amount of pre-strain comes back to its original shape and not more. Also, several numerical examples upon effect of different thermal condition, different volume fraction of SMA wires and different boundary conditions have been analyzed.

ARTICLE HISTORY
Received 31 October 2017
Accepted 31 October 2017

KEYWORDS
Carrera's Unified Formulation; multilayer composite plate; nonlinear dynamic analysis; Shape memory alloys; thermal loading

1. Introduction

Shape Memory Alloy materials, due to their unique mechanical behavior like shape memory effect, pseudoelastic effect and also temperature-dependent material properties, show great benefit as tools for improving the mechanical properties of structures. The ability to change and then recover a large strain is a result of a reversible martensite phase transformation due to the temperature or stress. Because of this transformation, shape memory alloys have some unique properties, such as superelasticity and recovery effects which lead to their wide aplication in the mechanical and aerospace engineering elements. The SMA fibers embedded inside composites can be employed for dynamical and structural vibration control. Parhi and singh [1] studied a nonlinear free vibration analysis cylindrical composite shell panels embedded with SMA fibers. They used the shape memory and stress recovery effect of SMA wires for improving the natural frequency of the composite shell. Lijun et al. [2] proposed a macro constitutive model which can be used to describe the mechanical behavior of FG-SMA under graded temperature loading. They found that the stress decreases due to the martensite transformation of SMA is remarkable. Botshekanan et al. [3]–[5] proposed a nonlinear finite element formulation for analysis of transient dynamic response of multilayered beam and plate embedded with SMA wires. They consider an instantaneous variation of martesite volume fraction and also material properties of the structures for the first time. They found a damped response of the structure due to the hysteresis loops of SMA wires. Eshghinejad and Elahinia [6] proposed an analytical approach to calculate the exact solution of SMA beams deflection due to an external force. Their model is appropriate for modeling of a SMA beam. Their results are validated with the existing plastic solution and experimental data.

Due to the shape memory effect of SMA's and therefore generating the stress recovery upon thermal conditions, the SMA wire are employed for improving the stiffness of structures, extensively. For example, Shiau et al. [7] studied the effect of shape memory alloys on the free vibration behavior of buckled cross-ply and angle-ply laminated plate by varying the SMA wire spacing. They showed that the increase of SMA wire volume fraction and pre-strain generate more recovery stress, and so increase the stiffness of SMA reinforced composite laminates. They noticed that the post-buckling deflections of the plate will be decreased considerably. Kabir and Tehrani [8] proposed a close form solution in order to study the thermal, mechanical, and thermomechanical buckling and post-buckling of symmetric laminated composite plates embedded SMA wires. They studied the effect of recovery stress of pre-strained SMA wires on the deformation of the plate. Khalili and Ardali [9]

Q2 **CONTACT** M. Botshekanan Dehkordi mbd_dehkordi@yahoo.com
Color versions of one or more of the figures in the article can be found online at www.tandfonline.com/umcm.

investigated the dynamic response of thin curved composite panel embedded with SMA wires subjected to low-velocity transverse impact. They used One-dimensional thermodynamic constitutive model proposed by Liang and Rogers for modelling the recovery stress in structure. Asadi et al. [10] studied the large amplitude vibration and thermal post-buckling of shape memory alloy wires reinforced hybrid composite beams with symmetric and asymmetric lay-up, analytically. They employed the one-dimensional Brinson SMA model, for modelling the recovery stress of SMA wires in the case of restrained strain. They investigate the effects of SMA wires parameters on the response of the structure. Asadi et al. [11] investigated the non-linear thermal instability of moving sandwich plates. They used the recovery stress of SMA wires for stabilizing the geometrically imperfection of the plate. They also employed the Brinson equation for modelling the recovery stress in SMA wires. Birman et al. [12] observed that if the SMA wires were embedded in the polymer composite plates, the recovery stresses are generated inside the structures and therefore, the impact resistance of the structures could be improved. In all of the researches reported above the recovery stress of SMA wires is modeled without considering the pseudoelastic effect of SMA wires. The reason is that the pseudoelastic effect make the behavior of SMA wires instantaneous and more complicated. Also in the researches done above, the recovery stress is modeled such that always increased with increasing the pre-strained of SMA wires. In this research this problems are removed during the modelling the behavior of SMA wires. Also in this research in order to robust analysis of the problem, the multilayered structures is modeled in the frame work of Carrera's Unified Formulation. In recent years, many theories proposed for analyzing the multilayer composite structures. Kirchhoff [13] (Classical laminate theory, CLT) and Reissner-Mindlin [14],[15] (First-order shear deformation theories, FSDT) plate theories are not suitable for the analysis of many multilayered structures [16]. They failed in order to fulfill the interlaminar transverse shear-stress continuity (IC) at each interface and to describe the so entitled zig-zag form of the displacement fields (ZZ) in the laminate thickness direction. In the recent years, Carrera et al. [17], [18]–[20] proposed a unified formulation (UF) of multilayered theories in the framework of both the PVD (Principle of Virtual Displacements) and RMVT (Reissner's mixed variational theorem) methods. This can be used as Equivalent-Single-Layer (ESL), if the variables are employed for the whole laminate, and also termed as Layer-Wise (LW), if the variables are used independently for each layer.

In this paper, the non-linear dynamic response of continuous composite plate embedded with pre-strained SMA wires is investigated considering the both effects of shape memory alloys simultaneously. The instantaneous phase transformation effects are considered at all the points on the plate. The constitutive equation of SMA proposed by Brinson is employed for modeling the effects of SMA wires. The models considered in this work are derived from the Reissner's Mixed Variational Theorem for modelling a priori the transverse shear and normal stresses. In this regard, the nonlinear strains are employed for modelling the thermal effects and also the effect of recovery stresses in the SMA wires. In this study not only the material properties are instantaneous variable with respect to the time and location, but they are also unknown, which make the problem more complicated. Therefore, a transient nonlinear finite element in conjunction with incremental iterative algorithm proposed by the author is employed, in order to solve the equations. Finally, the problem is coded in MATLAB software for studying the both effects of SMA wires on dynamic response of the SMA hybrid composite plate.

2. Constitutive model for the SMA wires

In this research, the one-dimensional constitutive model of SMA proposed by Brinson is employed. The constitutive model of Brinson [21] relates the stress (σ) to the strain (ε), temperature (T) and martensite fraction (ξ) as follows:

$$\sigma - \sigma_0 = E(\xi)(\varepsilon) - E(\xi_0)(\varepsilon_0) + \Omega(\xi)(\xi_s) - \Omega(\xi_0)(\xi_{s0}) \\ + \Theta(T - T_0) \tag{1}$$

Where $E(\xi)$, Θ and $\Omega(\xi)$ are Young's modulus, the thermoelastic tensor, and the transformation tensor, respectively. The terms associated with index "o" refer to the initial conditions. In addition, $E(\xi)$ and $\Omega(\xi)$ are defined as:

$$E(\xi) = E_A + \xi(E_M - E_A) \tag{2a}$$

$$\Omega(\xi) = -\varepsilon_L E(\xi) \tag{2b}$$

Where E_A and E_M are Young's modulus of SMA in austenite and martensite phases, respectively and ε_L is maximum recoverable strain. In this model, a modified cosine relation for the martensite volume fraction is separated as.

$$\xi = \xi_T + \xi_s \tag{3}$$

Where ξ_s represents the fraction of the material that is stress-induced martensite with single variants, and ξ_T denotes the fraction of the material that is temperature-induced martensite with multiple variant.Phase transformation's kinetic equations presented as:

2.1. Conversion to detwinned martensite

For $T > M_s$ and $\sigma_s^{cr} + C_M(T - M_s) < \sigma < \sigma_f^{cr} + C_M (T - M_s)$

$$\xi_s = \frac{1-\xi_{s0}}{2} \times \cos\left(\frac{\pi}{\sigma_s^{cr} - \sigma_f^{cr}}\left(\sigma - \sigma_f^{cr} - C_M\,(T - M_s)\right)\right) \\ + \frac{1+\xi_{s0}}{2}$$

$$\xi_T = \xi_{T0} - \frac{\xi_{T0}}{1-\xi_{s0}}(\xi_s - \xi_{s0}) \tag{4a}$$

For $T < M_s$ and $\sigma_s^{cr} < \sigma < \sigma_f^{cr}$

$$\xi_s = \frac{1-\xi_{s0}}{2} \times \cos\left(\frac{\pi}{\sigma_s^{cr} - \sigma_f^{cr}}\left(\sigma - \sigma_f^{cr}\right)\right) + \frac{1+\xi_{s0}}{2}$$

$$\xi_T = \xi_{T0} - \frac{\xi_{T0}}{1-\xi_{s0}}(\xi_s - \xi_{s0}) + \Delta_{T\xi} \tag{4b}$$

For $\mathrm{M_f} < T < \mathrm{M_s}$ and $\mathrm{T} < \mathrm{T_0}$

$$\Delta_{T\xi} = \frac{1-\xi_{T0}}{2}(\cos(a_M(T-M_f))+1)$$

Else $\Delta_{T\xi} = 0$

2.2. Conversion to austenite

For $\mathrm{T} > \mathrm{A_s}$ and $C_A(T-A_f) < \sigma < C_A(T-A_s)$

$$\begin{aligned} \xi &= \frac{\xi_0}{2}\cos\left(a_A\left(T-A_s-\frac{\sigma}{C_A}\right)+1\right) \\ \xi_s &= \xi_{s0} - \frac{\xi_{s0}}{\xi_0}(\xi_0-\xi) \\ \xi_T &= \xi_{T0} - \frac{\xi_{T0}}{\xi_0}(\xi_0-\xi) \end{aligned} \tag{4c}$$

In the above equations, σ_s^{cr} is the critical stress for the start of transformation and σ_f^{cr} is the critical stress at the end of transformation.

3. Unified formulation and finite element analysis

The Carrera's Unified Formulation (CUF) allows to handle many theories for plates and shells, by using the separation of the unknown variables into thickness functions (coordinate z), and the in-plane coordinates (x, y) functions [17]. In the framework of Carrera's unified formulation, the generic variable $\mathbf{a}(x, y, z)$ and its variation $\delta\mathbf{a}(x, y, z)$ can be expressed as bellow [17]:

$$\begin{aligned} &\mathbf{a}(x,y,z) = F_\tau(z)\mathbf{a}_\tau(x,y), \quad \delta\mathbf{a}(x,y,z) = F_s(z)\delta\mathbf{a}_s(x,y) \\ &with \quad \tau, s = t, b, r \quad and \quad r = 2,\ldots,N \end{aligned} \tag{5}$$

Bold letters imply arrays and the summing convention is defined with repeated indices τ and s. Subscripts t and b are corresponding to the top and bottom values. Also, r stand for the higher order terms of the expansion. The order of expansion N can be expanded from first to fourth order. Functions $F_\tau(\zeta_k)$ are thickness functions for the k^{th} layer. The Legendre polynomials $P_j(\zeta_k)$ are explained as follows:

$$\begin{aligned} &P_0 = 1, \quad P_1 = \zeta_k, \quad P_2 = \frac{(3\zeta_k{}^2-1)}{2}, \quad P_3 = \frac{5\zeta_k{}^3}{2} - \frac{3\zeta_k}{2}, \\ &P_4 = \frac{35\zeta_k{}^4}{8} - \frac{15\zeta_k{}^2}{4} + \frac{3}{8} \end{aligned} \tag{6}$$

where $\zeta_k = 2z_k/h_k$, while z_k and h_k imply the local coordinate and the thickness, which both are referred to k^{th} layer, therefore $-1 \le \zeta_k \le 1$. The thickness functions are expressed by combination the Legendre polynomials as bellow [17]:

$$F_t = \frac{P_0+P_1}{2}, \quad F_t = \frac{P_0-P_1}{2}, \quad F_r = P_r - P_{r-2}, \quad r = 2, 3, \ldots, N \tag{7}$$

These functions have the following properties:

$$\zeta_k = \begin{cases} 1, & F_t = 1,\ F_b = 0,\ F_r = 0 \\ -1, & F_t = 0,\ F_b = 1,\ F_r = 0 \end{cases} \tag{8}$$

These are the interface values of the variables that are defined as unknowns. This description can be used for both displacement $\mathbf{u} = (u_x, u_y, u_z)$ and transverse stresses $\sigma_n = (\sigma_{xz}, \sigma_{yz}, \sigma_{zz})$ components. According to this formulation, a corresponding model can be ESL when the variables are employed for the whole multilayer and LW when the variables are employed for each layer individually. The layer-wise models allow to impose the interlaminar continuity conditions, as bellow:

$$\mathbf{a}_t^k = \mathbf{a}_b^{k+1}, \quad k = 1,\ldots,N_l - 1 \tag{9}$$

where N_l is the number of the layers of the plate. The transverse stresses are always described as LW for reaching the interlaminar continuity conditions, while the displacement descriptions can be ESL or LW. In this study a quadratic nine-nodes finite element is used in order to approximate the displacements and the transverse stresses as bellow:

$$\mathbf{u}^k = F_\tau N_i \mathbf{q}_{\tau i}^k \qquad \sigma_{nM}^k = F_\tau N_i \mathbf{g}_{\tau i}^k \quad (i = 1,\ldots,9) \tag{10}$$

where N_i are the Lagrange quadratic shape functions, and:

$$\mathbf{q}_{\tau i}^k = \left[q_{u_x\tau i}^k \quad q_{u_y\tau i}^k \quad q_{u_z\tau i}^k\right]^T \qquad \mathbf{g}_{\tau i}^k = \left[g_{u_x\tau i}^k \quad g_{u_y\tau i}^k \quad g_{u_z\tau i}^k\right]^T \quad (i = 1,\ldots,N_n) \tag{11}$$

$\mathbf{q}_{\tau i}^k$ and $\mathbf{g}_{\tau i}^k$ are the nodal unknown of the element of the k^{th} layer.

4. Finite element formulation

The principle of Hamilton, can be expressed as:

$$\delta L_{\text{int}} - \delta L_{F_{in}} - \delta L_{ext} = 0 \tag{12}$$

where, L_{int} is the internal work, $L_{F_{in}}$ is the work done by the inertial force and L_{ext} is the work of the external force. The total internal work is devided to the mechanical work, work due to the phase transformation and also work of the thermal stress respectively as bellow:

$$L_{\text{int}} = L_{\text{int}M} + L_{\text{int}SMA} + L_{\text{int}T} \tag{13}$$

In this paper, the governing equations are derived using the Reissner's mixed variational theorem (RMVT) for satisfying the interlaminar continuity of transverse stresses between the layers [17], [18]. For study of sandwich plate with multilayered face-sheets embedded with pre-strained SMA wires, the RMVT is explained as bellow:

$$\begin{aligned} \delta(L_{\text{int}M} + L_{\text{int}T}) = \sum_{k=1}^{N_l}\int_{\Omega_k}\int_{A_k}\Big\{&\delta\varepsilon_{pG}^{k\ T}(\xi)\sigma_{pC}^k(\xi) \\ &+\delta\varepsilon_{nG}^{k\ T}(\xi)\sigma_{nM}^k(\xi) + \delta\sigma_{nM}^{k\ T}(\xi)(\varepsilon_{nG}^k(\xi) \\ &-\varepsilon_{nC}^k(\xi))\Big\}d\Omega dz_k \end{aligned} \tag{14}$$

In the framework of CUF, the linear strain components are explained as bellow:

$$\varepsilon_{pG}^k(\xi) = \{\varepsilon_{xx}(\xi),\ \varepsilon_{yy}(\xi),\ \varepsilon_{xy}(\xi)\}^{kT} = \mathbf{D}_p\ \mathbf{u}^k(\xi) \tag{15a}$$

$$\varepsilon_{nG}^k(\xi) = \{\gamma_{xz}(\xi),\ \gamma_{yz}(\xi),\ \varepsilon_{zz}(\xi)\}^{kT} = (\mathbf{D}_{np} + \mathbf{D}_{nz})\ \mathbf{u}^k(\xi) \tag{15b}$$

where the indices p and n mean the in-plane and normal components, respectively. The differential matrices are expressed as bellow:

$$\mathbf{D}_p = \begin{bmatrix} \partial_x & 0 & 0 \\ 0 & \partial_y & 0 \\ \partial_y & \partial_x & 0 \end{bmatrix}, \quad \mathbf{D}_{np} = \begin{bmatrix} 0 & 0 & \partial_x \\ 0 & 0 & \partial_y \\ 0 & 0 & 0 \end{bmatrix},$$

$$\mathbf{D}_{nz} = \begin{bmatrix} \partial_z & 0 & 0 \\ 0 & \partial_z & 0 \\ 0 & 0 & \partial_z \end{bmatrix} \tag{16}$$

Also, the 3D constitutive relations between the stress, strain and temperature are described as bellow:

$$\sigma_p^k(\xi) = \mathbf{C}_{pp}^k(\xi)\varepsilon_p^k(\xi) + \mathbf{C}_{pn}^k(\xi)\varepsilon_n^k(\xi) - \lambda_p^k(\xi)\theta \tag{17a}$$

$$\sigma_n^k(\xi) = \mathbf{C}_{np}^k(\xi)\varepsilon_p^k(\xi) + \mathbf{C}_{nn}^k(\xi)\varepsilon_n^k(\xi) - \lambda_n^k(\xi)\theta \tag{17b}$$

where σ_p^k, σ_p^k and $\mathbf{C}_{pp}^k$, $\mathbf{C}_{pn}^k$, $\mathbf{C}_{np}^k$ and $\mathbf{C}_{nn}^k$ are:

$$\begin{aligned} \sigma_p^k(\xi) &= \left\{\sigma_{xx}^k(\xi),\ \sigma_{yy}^k(\xi),\ \sigma_{xy}^k(\xi)\right\}, \\ \sigma_n^k(\xi) &= \left\{\sigma_{xz}^k(\xi),\ \sigma_{yz}^k(\xi),\ \sigma_{zz}^k(\xi)\right\} \end{aligned} \tag{18a}$$

$$\begin{aligned} \mathbf{C}_{pp}^k(\xi) &= \begin{bmatrix} C_{11}^k(\xi) & C_{12}^k(\xi) & C_{16}^k(\xi) \\ C_{12}^k(\xi) & C_{22}^k(\xi) & C_{26}^k(\xi) \\ C_{16}^k(\xi) & C_{26}^k(\xi) & C_{66}^k(\xi) \end{bmatrix}, \\ \mathbf{C}_{pn}^k(\xi) &= \begin{bmatrix} 0 & 0 & C_{13}^k(\xi) \\ 0 & 0 & C_{23}^k(\xi) \\ 0 & 0 & C_{36}^k(\xi) \end{bmatrix} \\ \mathbf{C}_{np}^k(\xi) &= \begin{bmatrix} 0 & 0 & 0 \\ 0 & 0 & 0 \\ C_{13}^k(\xi) & C_{23}^k(\xi) & C_{36}^k(\xi) \end{bmatrix}, \\ \mathbf{C}_{nn}^k(\xi) &= \begin{bmatrix} C_{55}^k(\xi) & C_{45}^k(\xi) & 0 \\ C_{45}^k(\xi) & C_{44}^k(\xi) & 0 \\ 0 & 0 & C_{33}^k(\xi) \end{bmatrix} \end{aligned} \tag{18b}$$

In the above relations Q^{kj} stands for the stiffness of the SMA hybrid composite for the k'th lamina of the sandwich plate and ξ is the martensite volume fraction. The material properties of a SMA hybrid composite lamina are evaluated as bellow [12]:

$$E_l(\xi) = E_l^c k_c + E_s(\xi)k_s \tag{19a}$$

$$\mathrm{E_t}(\xi) = \mathrm{E_t^c} / \left(1 - \sqrt{.\mathrm{k_s}}\left(1 - \mathrm{E_t^c}/\mathrm{E_s}(\xi)\right)\right) \tag{19b}$$

$$G_{lt}(\xi) = G_{lt}^c G_s(\xi)/(k_c G_s(\xi) + k_s G_{lt}^c) \tag{19c}$$

$$\upsilon_{lt} = \upsilon_{lt}^c k_c + \upsilon_s k_s \tag{19d}$$

where indices 's' and 'c' imply the SMA and the composite medium material, respectively. In the Eqs. (17) θ is the difference of temperature with respect to the reference temperature T_0. In the frame work of CUF, θ can be written as bellow:

$$\begin{aligned} &\theta^k = F_t\theta_t^k + F_b\theta_b^k + F_r\theta_r^k = F_\tau\theta_\tau^k \quad \tau = t, b, r, \\ &r = 2, \ldots, N, \quad k = 1, 2, \ldots, N_l \end{aligned} \tag{20}$$

Also, parameters λ_p^k and λ_n^k are expressed by the following form:

$$\begin{aligned} \lambda_p^k = \lambda_{pp}^k + \lambda_{pn}^k &= \begin{bmatrix} C_{11}^k(\xi) & C_{12}^k(\xi) & C_{16}^k(\xi) \\ C_{12}^k(\xi) & C_{22}^k(\xi) & C_{26}^k(\xi) \\ C_{16}^k(\xi) & C_{26}^k(\xi) & C_{66}^k(\xi) \end{bmatrix} \begin{bmatrix} \alpha_1^k \\ \alpha_2^k \\ \alpha_6^k \end{bmatrix} \\ &+ \begin{bmatrix} 0 & 0 & C_{13}^k(\xi) \\ 0 & 0 & C_{23}^k(\xi) \\ 0 & 0 & C_{36}^k(\xi) \end{bmatrix} \begin{bmatrix} 0 \\ 0 \\ \alpha_3^k \end{bmatrix} \end{aligned} \tag{21a}$$

$$\begin{aligned} \lambda_n^k = \lambda_{np}^k + \lambda_{nn}^k &= \begin{bmatrix} 0 & 0 & 0 \\ 0 & 0 & 0 \\ C_{13}^k(\xi) & C_{23}^k(\xi) & C_{36}^k(\xi) \end{bmatrix} \begin{bmatrix} \alpha_1^k \\ \alpha_2^k \\ \alpha_6^k \end{bmatrix} \\ &+ \begin{bmatrix} C_{55}^k(\xi) & C_{45}^k(\xi) & 0 \\ C_{45}^k(\xi) & C_{44}^k(\xi) & 0 \\ 0 & 0 & C_{33}^k(\xi) \end{bmatrix} \begin{bmatrix} 0 \\ 0 \\ \alpha_3^k \end{bmatrix} \end{aligned} \tag{21b}$$

where $\alpha_i^k(i = 1, 2, 3, 6)$ are thermal expansion coefficients. Above relations can be explained in the compact form as bellow:

$$\lambda_p^k(\xi) = \lambda_{pp}^k(\xi) + \lambda_{pn}^k(\xi) = \mathbf{C}_{pp}^k(\xi)\alpha_p^k + \mathbf{C}_{pn}^k(\xi)\alpha_n^k \tag{22a}$$

$$\lambda_n^k(\xi) = \lambda_{np}^k(\xi) + \lambda_{nn}^k(\xi) = \mathbf{C}_{np}^k(\xi)\alpha_p^k + \mathbf{C}_{nn}^k(\xi)\alpha_n^k \tag{22b}$$

In RMVT the displacements and transverse stresses are unknowns and so the constitutive Eqs. (17) must be rewritten as bellow:

$$\sigma_{pC}^k(\xi) = \tilde{\mathbf{C}}_{pp}^k(\xi)\varepsilon_{pG}^k(\xi) + \tilde{\mathbf{C}}_{pn}^k(\xi)\sigma_{nM}^k(\xi) + \tilde{\lambda}_p^k(\xi)\theta \tag{23a}$$

$$\varepsilon_{nC}^k(\xi) = \tilde{\mathbf{C}}_{np}^k(\xi)\varepsilon_{pG}^k(\xi) + \tilde{\mathbf{C}}_{nn}^k(\xi)\sigma_{nM}^k(\xi) + \tilde{\lambda}_n^k(\xi)\theta \tag{23b}$$

In theses equations, the new coefficients are explained as bellow:

$$\begin{aligned} \tilde{\mathbf{C}}_{pp}^k(\xi) &= \mathbf{C}_{pp}^k(\xi) - \mathbf{C}_{pn}^k(\xi)\mathbf{C}_{nn}^{k-1}(\xi)\mathbf{C}_{np}^k(\xi) \\ \tilde{\mathbf{C}}_{pn}^k(\xi) &= \mathbf{C}_{pn}^k(\xi)\mathbf{C}_{nn}^{k-1}(\xi) \end{aligned} \tag{24a}$$

$$\begin{aligned} \tilde{\mathbf{C}}_{np}^k(\xi) &= -\mathbf{C}_{nn}^{k-1}(\xi)\mathbf{C}_{np}^k(\xi) \\ \tilde{\mathbf{C}}_{nn}^k(\xi) &= -\mathbf{C}_{nn}{}^{k-1}(\xi) \end{aligned} \tag{24b}$$

$$\begin{aligned} \tilde{\lambda}_p^k(\xi) &= \mathbf{C}_{pn}^k(\xi)\mathbf{C}_{nn}^{k-1}(\xi)\lambda_n^k(\xi) - \lambda_p^k(\xi) \\ \tilde{\lambda}_n^k(\xi) &= \mathbf{C}_{nn}^{k-1}(\xi)\lambda_n^k(\xi) \end{aligned} \tag{24c}$$

By substituting Eqs. (23) in Eq. (14), we have:

$$\begin{aligned} \delta(L_{\mathrm{int}M} + L_{\mathrm{int}T}) = \sum_{k=1}^{N_l} \int_{\Omega_k}\int_{A_k} \Bigg\{ & \underbrace{\delta\varepsilon_{pG}^{k\ T}\tilde{\mathbf{C}}_{pp}^k\varepsilon_{pG}^k}_{I} \\ &+ \underbrace{\delta\varepsilon_{pG}^{k\ T}\tilde{\mathbf{C}}_{pn}^k\sigma_{nM}^k}_{II} + \underbrace{\delta\varepsilon_{nG}^{k\ T}\sigma_{nM}^k}_{III} + \underbrace{\delta\sigma_{nM}^{k\ T}\varepsilon_{nG}^k}_{IV} \\ &- \underbrace{\delta\sigma_{nM}^{k\ T}\tilde{\mathbf{C}}_{np}^k\varepsilon_{pG}^k}_{V} - \underbrace{\delta\sigma_{nM}^{k\ T}\tilde{\mathbf{C}}_{nn}^k\sigma_{nM}^k}_{VI} \\ &+ \underbrace{\delta\varepsilon_{pG}^{k\ T}\lambda_p^{k\theta}\theta^k}_{VII} - \underbrace{\delta\sigma_{nM}^{k\ T}\lambda_n^{k\theta}\theta^k}_{VIII} \Bigg\} d\Omega dz_k \end{aligned} \tag{25}$$

where the terms *I-VI* are related to the mechanical work and the terms *VII* and *VIII* are the work done by the thermal stress; therefore it can be found:

$$\delta L_{\mathrm{int}M} = \sum_{k=1}^{N_l} \int_{\Omega_k} \int_{A_k} \{ \delta \varepsilon_{pG}^{k\ T} \tilde{\mathbf{C}}_{pp}^k \varepsilon_{pG}^k + \delta \varepsilon_{pG}^{k\ T} \tilde{\mathbf{C}}_{pn}^k \sigma_{nM}^k + \delta \varepsilon_{nG}^{k\ T} \sigma_{nM}^k + \delta \sigma_{nM}^{k\ T} \varepsilon_{nG}^k - \delta \sigma_{nM}^{k\ T} \tilde{\mathbf{C}}_{np}^k \varepsilon_{pG}^k - \delta \sigma_{nM}^{k\ T} \tilde{\mathbf{C}}_{nn}^k \sigma_{nM}^k \} d\Omega dz_k \tag{26a}$$

$$\delta L_{\mathrm{int}T} = \sum_{k=1}^{N_l} \int_{\Omega_k} \int_{A_k} \left\{ \delta \varepsilon_{pG}^{k\ T} \tilde{\lambda}_p^k \theta^k - \delta \sigma_{nM}^{k\ T} \tilde{\lambda}_n^k \theta^k \right\} d\Omega dz_k \tag{26b}$$

By substituting Eqs. (10), (11) and (15) in Eq. (26a), we have:

$$\begin{aligned} \delta L_{\mathrm{int}M}^k = & \lhd \left\{ \delta \mathbf{q}_{\tau i}^{kT}(\xi) \left[\mathbf{D}_p^T (N_i \mathbf{I}) \tilde{\mathbf{Z}}_{pp}^{k\tau s}(\xi) \mathbf{D}_p^T (N_j \mathbf{I}) \right] \mathbf{q}_{sj}^k(\xi) \right\} \rhd_\Omega + \\ & + \lhd \left\{ \delta \mathbf{q}_{\tau i}^{kT}(\xi) \left[\mathbf{D}_p^T (N_i \mathbf{I}) \tilde{\mathbf{Z}}_{pn}^{k\tau s}(\xi) N_j \right] \mathbf{g}_{sj}^k(\xi) \right\} \rhd_\Omega + \\ & + \lhd \left\{ \delta \mathbf{q}_{\tau i}^{kT}(\xi) \left[\mathbf{D}_{n\Omega}^T (N_i \mathbf{I}) E_{\tau s} N_j + E_{\tau_{,z} s} N_i N_j \mathbf{I} \right] \mathbf{g}_{sj}^k(\xi) \right\} \rhd_\Omega + \\ & + \lhd \left\{ \delta \mathbf{g}_{\tau i}^{kT}(\xi) \left[N_i E_{\tau s} \mathbf{D}_{n\Omega} (N_j \mathbf{I}) + E_{\tau s_{,z}} N_i N_j \mathbf{I} \right] \mathbf{q}_{sj}^k(\xi) \right\} \rhd_\Omega + \\ & - \lhd \left\{ \delta \mathbf{g}_{\tau i}^{kT}(\xi) \left[N_i \tilde{\mathbf{Z}}_{np}^{k\tau s}(\xi) \mathbf{D}_p (N_j \mathbf{I}) \right] \mathbf{q}_{sj}^k(\xi) \right\} \rhd_\Omega + \\ & - \lhd \left\{ \delta \mathbf{g}_{\tau i}^{kT}(\xi) \left[N_i \tilde{\mathbf{Z}}_{nn}^{k\tau s}(\xi) N_j \right] \mathbf{g}_{sj}^k(\xi) \right\} \rhd_\Omega \end{aligned} \tag{27}$$

where the layer's stiffness and compliance are obtained as bellow:

$$\left(\tilde{\mathbf{Z}}_{pp}^{k\tau s}(\xi), \tilde{\mathbf{Z}}_{pn}^{k\tau s}(\xi), \tilde{\mathbf{Z}}_{np}^{k\tau s}(\xi), \tilde{\mathbf{Z}}_{nn}^{k\tau s}(\xi) \right) = \left(\tilde{\mathbf{C}}_{pp}^k(\xi), \tilde{\mathbf{C}}_{pn}^k(\xi), \tilde{\mathbf{C}}_{np}^k(\xi), \tilde{\mathbf{C}}_{nn}^k(\xi) \right) E_{\tau s} \tag{28}$$

The symbols $\lhd \ldots \rhd_\Omega$ means the integrals on the domain Ω. The integration in the thickness direction can be evaluated as bellow:

$$E_{\tau s}, E_{\tau_{,z} s}, E_{\tau s_{,z}} = \int_{A_k} (F_\tau F_s, F_{\tau_{,z}} F_s, F_\tau F_{s_{,z}}) dz \tag{29}$$

And therefore the Eq. (27) can be rewritten as bellow:

$$\begin{aligned} \delta L_{\mathrm{int}M}^k = & \delta \mathbf{q}_{\tau i}^{kT}(\xi) \left[\mathbf{K}_{uu}^{k\tau sij}(\xi) \mathbf{q}_{sj}^k(\xi) + \mathbf{K}_{u\sigma}^{k\tau sij}(\xi) \mathbf{g}_{sj}^k(\xi) \right] \\ & + \delta \mathbf{g}_{\tau i}^{kT}(\xi) \left[\mathbf{K}_{\sigma u}^{k\tau sij}(\xi) \mathbf{q}_{sj}^k(\xi) + \mathbf{K}_{\sigma\sigma}^{k\tau sij}(\xi) \mathbf{g}_{sj}^k(\xi) \right] \end{aligned} \tag{30}$$

where

$$\mathbf{K}_{uu}^{k\tau sij}(\xi) = \lhd \left[\mathbf{D}_p^T (N_i \mathbf{I}) \tilde{\mathbf{Z}}_{pp}^{k\tau s}(\xi) \mathbf{D}_p^T (N_j \mathbf{I}) \right] \rhd_\Omega \tag{31a}$$

$$\mathrm{E_t}(\xi) = \mathrm{E_t^c} / \left(1 - \sqrt{\mathrm{k_s}} (1 - \mathrm{E_t^c}/\mathrm{E_s}(\xi)) \right) \tag{31b}$$

$$\mathbf{K}_{\sigma u}^{k\tau sij}(\xi) = \lhd \left[N_i E_{\tau s} \mathbf{D}_{n\Omega} (N_j \mathbf{I}) + E_{\tau s_{,z}} N_i N_j \mathbf{I} - N_i \tilde{\mathbf{Z}}_{np}^{k\tau s}(\xi) \mathbf{D}_p (N_j \mathbf{I}) \right] \rhd_\Omega \tag{31c}$$

$$\mathbf{K}_{\sigma\sigma}^{k\tau sij}(\xi) = \lhd \left[- N_i \tilde{\mathbf{Z}}_{nn}^{k\tau s}(\xi) N_j \right] \rhd_\Omega \tag{31d}$$

Above components are [3 × 3] 'fundamental nuclei' that the stiffness matrices of the whole plate can be obtained by expanding and assembling them through the indices *k;τ; s; i; j*. The explicit form of this nucleus are explained in appendix.

Due to the the location dependency of the coefficients $\tilde{\mathbf{Z}}_{ij}^{k\tau s}(\xi)(i, j = p, n)$, they must be stay in the integral domain. The integrals in the surface and in the thickness direction are evaluated numerically using the Gaussian quadrature method. The selective reduced integration is employed at layer-level in order to overcome the shear locking effect [18]. In this research, for obtaining the work done by the thermal stress, the nonlinear strain components are employed. Therefore, the Eq. (26b) is rewritten as bellow:

$$\delta L_{\mathrm{int}T} = \sum_{k=1}^{N_l} \int_{\Omega_k} \int_{A_k} \left\{ \delta \varepsilon_{pG_{nl}}^{k\ T} \tilde{\lambda}_p^k \theta^k - \delta \sigma_{nM}^{k\ T} \tilde{\lambda}_n^k \theta^k \right\} d\Omega dz_k \tag{32}$$

where $\varepsilon_{pG_{nl}}^k$ stand for the nonlinear in-plane strain components which can be explained as bellow:

$$\varepsilon_{pG_{nl}}^k(\xi) = \{ \varepsilon_{xx_{nl}}(\xi),\ \varepsilon_{yy_{nl}}(\xi),\ \varepsilon_{xy_{nl}}(\xi) \}^{kT} = \mathbf{D}_{p_{nl}} \mathbf{u}^k(\xi) \tag{33}$$

where

$$\mathbf{D}_{p_{nl}} = \begin{bmatrix} \partial_x & 0 & \frac{1}{2} \partial^2{}_{x^2} \\ 0 & \partial_y & \frac{1}{2} \partial^2{}_{y^2} \\ \partial_y & \partial_x & \partial^2{}_{xy} \end{bmatrix} \tag{34}$$

By substituting Eqs. (10), (20) and (33) in Eq. (32), it can be found:

$$\delta L_{\mathrm{int}T} = \delta \mathbf{q}_{\tau i}^{kT}(\xi) \left(\mathbf{P}_{u\theta\tau i}^k + \mathbf{K}_{uu_{nlT}}^{k\tau sij}(\xi) \right) + \delta \mathbf{g}_{\tau i}^{kT}(\xi) \mathbf{P}_{\sigma\theta\tau i}^k \tag{35}$$

where

$$\mathbf{P}_{u\theta\tau i}^k = \begin{bmatrix} P_{u\theta\tau i11}^k \\ P_{u\theta\tau i21}^k \\ P_{u\theta\tau i31}^k \end{bmatrix}, \quad \mathbf{P}_{\sigma\theta}^k = \begin{bmatrix} P_{\sigma\theta\tau i11}^k \\ P_{\sigma\theta\tau i21}^k \\ P_{\sigma\theta\tau i31}^k \end{bmatrix} \tag{36}$$

The components of the above relations are explained as bellow:

$$\begin{aligned} P_{u\theta\tau i11}^{ki} &= E_{\tau s} \lhd [N_{i,x} N_j] \rhd_\Omega k_c^k \tilde{\lambda}_{p1}^k \theta_{sj}^k + E_{\tau s} \lhd [N_{i,y} N_j] \rhd_\Omega k_c^k \tilde{\lambda}_{p3}^k \theta_{sj}^k \\ P_{u\theta\tau i21}^k &= E_{\tau s} \lhd [N_{i,y} N_j] \rhd_\Omega k_c^k \tilde{\lambda}_{p2}^k \theta_{sj}^k + E_{\tau s} \lhd [N_{i,x} N_j] \rhd_\Omega k_c^k \tilde{\lambda}_{p3}^k \theta_{sj}^k \\ P_{u\theta\tau i31}^k &= 0 \\ P_{\sigma\theta\tau i11}^k &= 0 \\ P_{\sigma\theta\tau i21}^k &= 0 \\ P_{\sigma\theta\tau i31}^k &= E_{\tau s} \lhd [N_i N_j] \rhd_\Omega k_c^k \tilde{\lambda}_{n3}^k \theta_{sj}^k \end{aligned} \tag{37}$$

where k_c^k is the volume fraction of the composite medium for the k'th layer of the structure and can be explained as bellow:

$$k_c^k = 1 - k_{Sx}^k - k_{Sy}^k \tag{38}$$

In the relation (38), $\mathrm{k_s^{kj}}$ indicate the volume fraction of the SMA wires in the k'th layer in the x and y directions, respectively. In the Eq. (35) $\mathbf{K}_{uu_{nl\theta}}^{k\tau sij}$ is the stiffness matrix due to the thermal effects and can be expressed as bellow:

$$\mathbf{K}_{uu_{nlT}}^{k\tau sij} = \begin{bmatrix} 0 & 0 & 0 \\ 0 & 0 & 0 \\ 0 & 0 & K_{uu_{nlT}zz}^{k\tau sij} \end{bmatrix} \tag{39}$$

where $K_{uu_{nlT}zz}^{k\tau s}$ can be evaluated as bellow:

$$K_{uu_{nlT}zz}^{k\tau sij} = -E_{\tau s} k_c^k \Big(\lhd [N_{i,x} N_{j,x}] \rhd_\Omega \tilde{\lambda}_{p1}^k + \lhd [N_{i,y} N_{j,y}] \rhd_\Omega \tilde{\lambda}_{p2}^k + \lhd [N_{i,x} N_{j,y} + N_{i,y} N_{j,x}] \rhd_\Omega \tilde{\lambda}_{p3}^k \Big) \theta^k \tag{40}$$

In this research, for evaluating the work due to the phase transformation in the SMA wires, the nonlinear strain components are used again. Therefore, $\delta L^k_{\mathrm{int}SMA}$ is described as bellow:

$$\delta L_{\mathrm{int}SMA} = \sum_{k=1}^{N_l} \int_{\Omega_k} \int_{A_k} \left\{ \delta \varepsilon^{k\;T}_{pG_{nl}}(\xi) \kappa^k(\xi) \right\} d\Omega dz_k \tag{41}$$

In the above relation $\kappa^k(\xi)$ is obtained as bellow:

$$\kappa^k(\xi) = \begin{bmatrix} k^k_{Sx}\chi^k_{Sx}(\xi) \\ k^k_{Sy}\chi^k_{Sy}(\xi) \\ 0 \end{bmatrix} \tag{42}$$

The new terms $\chi^k_{Si}(\xi)(i = x, y)$ are the effect of phase transformation in the SMA wires in the x and y directions, respectively, which can be explained as bellow:

$$\chi^k_{Sx}(\xi) = E^k_{Sx}(\xi^k_x)\varepsilon_0 - \varepsilon_L E^k_{Sx}(\xi^k_x)\xi^k_x + \vartheta(\theta^k - \theta^k_0) \tag{43a}$$

$$\chi^k_{Sy}(\xi) = E^k_{Sy}(\xi^k_y)\varepsilon_0 - \varepsilon_L E^k_{Sy}(\xi^k_y)\xi^k_y + \vartheta(\theta^k - \theta^k_0) \tag{43b}$$

where ξ^{kj} and E^{kj}_s imply the martensite volume fraction and the Young's modulus of the SMA wires of the k'th lamina, respectively. By substituting Eqs. (10), (33) and (42) in Eq. (41), it can be written:

$$\delta L_{\mathrm{int}SMA} = \delta \mathbf{q}^{kT}_{\tau i}(\xi)(\mathbf{P}^k_{sma\tau i}(\xi) + \mathbf{K}^{k\tau sij}_{uu_{nlSMA}}(\xi)) \tag{44}$$

where

$$\mathbf{P}^k_{sma\tau i}(\xi) = \begin{bmatrix} P^k_{sma\tau i11}(\xi) \\ P^k_{sma\tau i21}(\xi) \\ 0 \end{bmatrix} \tag{45}$$

The components of the above relation are explained as bellow:

$$P^{ki}_{sma\tau i11} = k^k_{Sx} E_\tau \triangleleft \left[N_{i,x}\chi^k_{Sx}(\xi) \right] \triangleright_\Omega \tag{46a}$$

$$P^{ki}_{sma\tau i21} = k^k_{Sy} E_\tau \triangleleft \left[N_{i,y}\chi^k_{Sy}(\xi) \right] \triangleright_\Omega \tag{46b}$$

In the above relation, E_τ is the integral through the thickness and can be obtained as bellow:

$$E_\tau = \int_{A_k} F_\tau dz \tag{47}$$

In the Eq. (44), $\mathbf{K}^{k\tau sij}_{uu_{nlSMA}}(\xi)$ is the stiffness matrix due to the effect of phase transformation (especially due to the recovery stress induced by the shape memory effect in the pre-strained SMA wires) and can be explained as bellow:

$$\mathbf{K}^{k\tau sij}_{uu_{nlSMA}}(\xi) = \begin{bmatrix} 0 & 0 & 0 \\ 0 & 0 & 0 \\ 0 & 0 & K^{k\tau sij}_{uu_{nlSMA}zz}(\xi) \end{bmatrix} \tag{48}$$

where $K^{k\tau sij}_{uu_{nlSMA}zz}(\xi)$ can be obtained as bellow:

$$K^{k\tau sij}_{uu_{nlSMA}zz}(\xi) = E_{\tau s}\big(k^k_{Sx}\triangleleft[N_{i,x}N_{j,x}\chi^k_{Sx}(\xi)]\triangleright_\Omega + k^k_{Sy}\triangleleft[N_{i,y}N_{j,y}\chi^k_{Sy}(\xi)]\triangleright_\Omega\big) \tag{49}$$

According to the CUF, $\delta L^k_{F_{in}}$ is explained as bellow:

$$\delta L^k_{F_{in}} = \delta \mathbf{q}^{kT}_{\tau i}(\xi)\mathbf{M}^{ksij}\ddot{\mathbf{q}}^k_{sj}(\xi) \tag{50}$$

where

$$\mathbf{M}^{k\tau sij} = \begin{bmatrix} m^k_{\tau s}\triangleleft[N_iN_j]\triangleright_\Omega & 0 & 0 \\ 0 & m^k_{\tau s}\triangleleft[N_iN_j]\triangleright_\Omega & 0 \\ 0 & 0 & m^k_{\tau s}\triangleleft[N_iN_j]\triangleright_\Omega \end{bmatrix} \tag{51}$$

and

$$m^k_{\tau s} = \int_{A_k} \rho^k F_\tau F_s dz \tag{52}$$

The method used to derive finite element stiffness/compliance matrices is employed to evaluate the work done by the external loads. For example, it is assumed that a distribution of pressure is done on the layer k, with distant $\zeta_k = \zeta^1_k$ from the reference surface. The external work done by this pressure is described as bellow:

$$\delta L^k_{ext} = \int_{\Omega_k} \delta \mathbf{u}^{kT}\left(x, y, \zeta^k_1\right) \mathbf{P}^k\left(x, y, \zeta^k_1\right) d\Omega \tag{53}$$

where

$$\mathbf{u}^k = F^1_\tau N_i \mathbf{q}^k_{\tau i} \quad (i = 1, 2, \ldots, N_n) \tag{54}$$

and $\boldsymbol{P}^k(x, y, \zeta^k_1)$ is the pressure and can be expanded as bellow:

$$\mathbf{P}^k = F^1_t\mathbf{P}^k_t + F^1_r\mathbf{P}^k_r + F^1_b\mathbf{P}^k_b = F^1_\tau\mathbf{P}^k_\tau, \quad \tau = t, b, r, \quad r = 2, 3, \ldots, N, \quad k = 1, 2, \ldots, N_l \tag{55}$$

where

$$\mathbf{P}^k_\tau = N_i \mathbf{p}^k_{\tau i} \quad (i = 1, 2, \ldots, N_n) \tag{56}$$

$\mathbf{p}^k_{\tau i}$ is explained as:

$$\mathbf{p}^k_{\tau i} = \begin{bmatrix} p^k_{x\tau i} & p^k_{y\tau i} & p^k_{z\tau i} \end{bmatrix}^T \tag{57}$$

Therefore:

$$\mathbf{P}^k = F^1_\tau N_i \mathbf{p}^k_{\tau i} \tag{58}$$

By substituting Eq. (54) and Eq. (58) in Eq. (53), we have:

$$\delta L^k_{ext} = \int_{\Omega_k} \delta \mathbf{q}^{kT}_{\tau i}(\xi)\left(F^1_\tau F^1_s\right)(N_iN_j)\mathbf{p}^k_{sj} d\Omega = \delta \mathbf{q}^{kT}_{\tau i}(\xi)\mathbf{P}^k_{\tau i} \tag{59}$$

where:

$$\mathbf{P}^k_{\tau i} = (F^1_\tau F^1_s)\begin{bmatrix} \triangleleft[N_iN_j]\triangleright_\Omega & p^k_{xsj} \\ \triangleleft[N_iN_j]\triangleright_\Omega & p^k_{ysj} \\ \triangleleft[N_iN_j]\triangleright_\Omega & p^k_{zsj} \end{bmatrix} \tag{60}$$

By substituting Eqs. (30), (35), (44), (50) and (59) in Eq. (12) the governing equations are explained as bellow:

$$\delta \mathbf{q}^{kT}_{\tau i}(\xi) : \mathbf{K}^{k\tau sij}_{uu}(\xi)\mathbf{q}^k_{sj}(\xi) + \mathbf{K}^{k\tau sij}_{u\sigma}(\xi)\mathbf{g}^k_{sj}(\xi) + \mathbf{M}^{ksij}\ddot{\mathbf{q}}^k_{sj}(\xi) = \mathbf{P}^k_{\tau i} - \mathbf{P}^k_{u\theta\tau i} - \mathbf{P}^k_{sma\,\tau i}(\xi) \tag{61a}$$

$$\delta \mathbf{g}^{kT}_{\tau i}(\xi) : \mathbf{K}^{k\tau sij}_{\sigma u}(\xi)\mathbf{q}^k_{sj}(\xi) + \mathbf{K}^{k\tau sij}_{\sigma\sigma}(\xi)\mathbf{g}^k_{sj}(\xi) = -\mathbf{P}^k_{\sigma\theta\tau i} \tag{61b}$$

In the Eq. (59a), $\mathbf{K}_{uu}^{k\tau sij}(\xi)$ is the total element stiffness of the k'th layer and can be explained as bellow:

$$\mathbf{K}_{uu}^{k\tau sij}(\xi)=\mathbf{K}_{uu_{mech}}^{k\tau sij}(\xi)+\mathbf{K}_{uu_{nlSMA}}^{k\tau sij}(\xi)+\mathbf{K}_{uu_{nl\theta}}^{k\tau sij}(\xi) \tag{62}$$

According to the governing equation, it must be noticed that stiffness/compliance matrices and also force vector are dependent on the martensite volume fraction and so these stiffness/compliance matrices are variable with time and also they are unknown. In other words, the governing equations of motion are coupled with the kinetic relations of phase transformation. Therefore, for solving the nonlinear equations, the incremental iterative technique proposed by the author (see Refs. [3]) is used. In this research the nodal stress unknown are eliminated by the 'static condensation' method. Therefore, the Eqs. (61) can be rewritten as bellow:

$$\mathbf{K}(\xi)\mathbf{q}(\xi)+\mathbf{M}\ddot{\mathbf{q}}(\xi)=\mathbf{P}(\xi) \tag{63}$$

where

$$\begin{aligned}\mathbf{K}(\xi)&=[\mathbf{K}_{uu}(\xi)-\mathbf{K}_{u\sigma}(\xi)\mathbf{K}_{\sigma\sigma}(\xi)^{-1}\mathbf{K}_{\sigma u}(\xi)],\\ \mathbf{P}(\xi)&=\mathbf{P}+\mathbf{K}_{u\sigma}(\xi)\mathbf{K}_{\sigma\sigma}(\xi)^{-1}\mathbf{P}_{\sigma\theta}-\mathbf{P}_{u\theta}-\mathbf{P}_{sma}(\xi)\end{aligned} \tag{64}$$

The Newmark method is used for the time integration of Eq. (63) with time as follows [22]:

$$\{q\}_{m+1}=\{\mathrm{q}\}_m+\Delta\mathrm{t}\{\dot{\mathrm{q}}\}_m+\frac{1}{2}\Delta\mathrm{t}^2\{\ddot{q}\}_{m+\gamma} \tag{65a}$$

$$\{\dot{\mathrm{q}}\}_{m+1}=\{q\}_m+\Delta\mathrm{t}\{\ddot{q}\}_{m+\alpha} \tag{65b}$$

where $\{q\}$ and $\{\dot{\mathrm{q}}\}$ are respectively the element displacement vector and its first derivative with respect to time. Also

$$\{\ddot{q}\}_{m+\alpha}=(1-\alpha)\{\ddot{q}\}_m+\alpha\{\ddot{q}\}_{m+1} \tag{65c}$$

Here $\alpha=\gamma=1/2$ [22]. The set of expressions in (63) can be reduced, with the help of Eqs. (65a)–(65c), to the discretized form of the element equation, as bellow:

$$\left[\hat{K}\right]_{m+1}\{q\}_{m+1}=\left\{\hat{\mathrm{F}}\right\}_{m,m+1} \tag{66}$$

where

$$[\hat{K}]_{m+1}=[K]_{m+1}+a_3[M]_{m+1} \tag{67a}$$

$$\left\{\hat{\mathrm{F}}\right\}_{m,m+1}=\{\mathrm{F}\}_{m,m+1}+[M]_{m+1}\left(a_3\{q\}_m+a_4\{\dot{\mathrm{q}}\}_m+a_5\{\ddot{q}\}_m\right) \tag{67b}$$

and a3, a4 and a5 are defined as [22]:

$$a_3=\frac{2}{\gamma(\Delta t)^2},\quad a_4=\frac{2}{\gamma\Delta t},\quad a_5=\frac{1}{\gamma}-1 \tag{68}$$

The initial value of acceleration is usually not known. As an approximation, it can be calculated from Eq. (63) using initial conditions on $\{q\}_0$ and $\{\mathrm{F}\}_0$ (often $\{\mathrm{F}\}$ is assumed to be zero at $\mathrm{t}=0$):

$$\{\ddot{q}\}_0=[M]^{-1}\left(\{\mathrm{F}^{\mathrm{e}}\}_0-[K]\{q\}_0\right) \tag{69}$$

At the end of each time step, the new velocity and acceleration vectors are computed using the following equations:

$$\{\ddot{q}\}_{m+1}=a_3\left(\{q\}_{m+1}-\{q\}_m\right)-a_4\{\dot{\mathrm{q}}\}_m-a_5\{\ddot{q}\}_m \tag{70a}$$

Table 1. Material properties of the composite and SMA wires [23].

Material	E(GPa)	υ	$\rho(\mathrm{kg/m^3})$
Epoxy resin	3.43	0.35	1250.0
Graphite fibers	275.6	0.2	1900.0
SMA-Martensite	26.3	0.3	6448.1
SMA-Austenite	67.0	0.3	6448.1

$$\{\dot{\mathrm{q}}\}_{m+1}=\{\dot{\mathrm{q}}\}_m+a_2\{\ddot{q}\}_m+a_1\{\ddot{q}\}_{m+1} \tag{70b}$$

where $a_1=\alpha\Delta t$ and $a_2=(1-\alpha)\Delta t$.

5. Numerical results

A new m-file program in MATLAB software is written in order to derivation the results based on the nonlinear finite element formulation explained above. First of all, for verification the effect of recovery stress or shape memory effect on the response of plate and also assessment the accuracy of the proposed finite element formulation, a composite multilayered plate embedded with pre-strained SMA wires is considered. Length and thickness of the plate are 500 mm and 9 mm, respectively [23]. The plate is made of 12 layers by which the two outer layers are SMA/epoxy and the other ten layers are graphite/epoxy. The thickness of each SMA/epoxy layer is 0.5 mm, and the volume fraction of SMA wire is 0.57. Also, the volume fraction of the graphite fibers in the graphite/epoxy layers is 0.5, and the thickness of each graphite/epoxy layer is 0.8 mm. The scheme lamination of the plate is$[0^\circ/(\pm45^\circ)_5/0^\circ]$. The material properties of the composite and the SMA wires are reported in Table 1. In this verification the variation of temperature is such that the generated recovery stresses in the SMA wires is about 172.1 MPa [23]. The relative natural frequency of the plate is sees in Figure 2 for different length to width ratios. It should be mentioned that the relative natural frequency means the ratio of the natural frequency of the plate, when the SMA wires are activated to the corresponding value when the SMA wires are not activated. As can be seen in Figure 2, a very good agreement is observed between the results of the present formulation and the results obtained by Zack et al. [23]. Also for verification of pseudoelastic effect of SMA wires, a transient dynamic analysis of the structure is done by the author in [23].

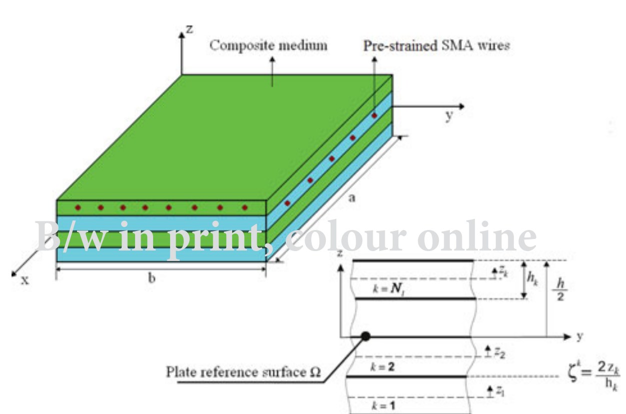

Q3

Figure 1. Geometry and coordinate systems of multilayered plate embedded with pre-strained SMA wires.

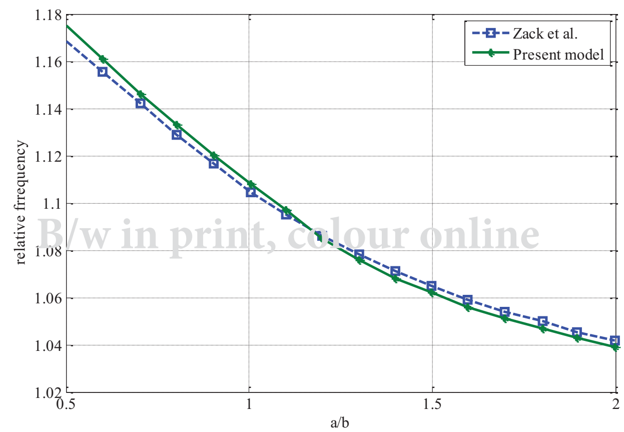

Figure 2. Variation of relative natural frequency with aspect ratio.

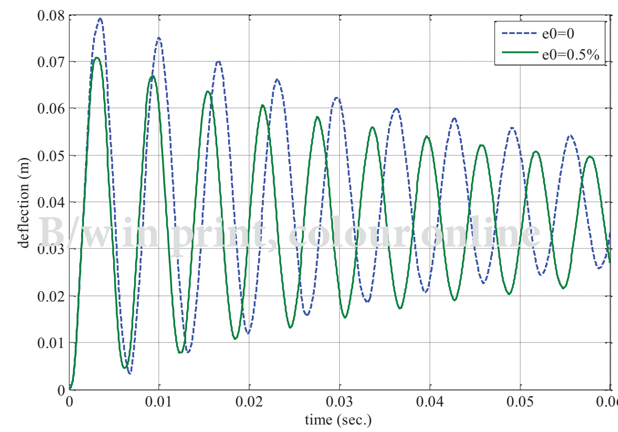

Figure 3. Response history of deflection at the center of the plate for thermal-mechanical loading.

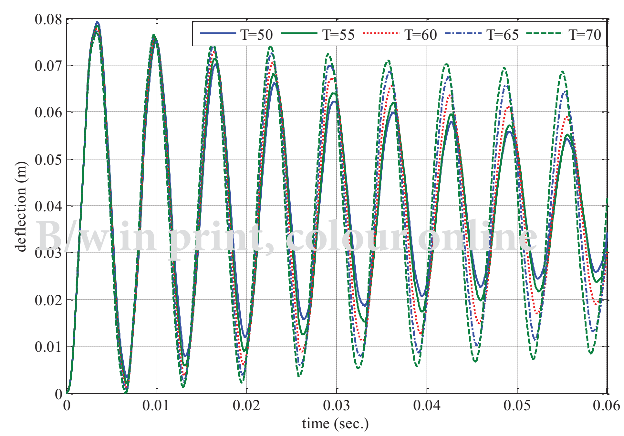

Figure 3. Response history of deflection at the center of the plate for different temperature (isothermal condition). Q5

Table 2. Material properties of shape memory alloys [21].

$E_a = 67$ GPa	$T = 50°C$	$C_M = 8$ $MPa/°C$
$E_M = 26.3$ GPa	$M_f = 9°C$	$C_A = 13.8$ MPa/°C
$\sigma_s^{cr} = 100$ MPa	$M_s = 18.4°C$	$\theta = 0.55$ $MPa/°C$
$\sigma_f^{cr} = 170$ MPa	$A_s = 34.5°C$	$\rho_s = 6500$ kg/m^3
$\varepsilon_L = 0.067$	$A_f = 49°C$	$\upsilon_s = 0.33$

In this part, a transient dynamic analysis of simply supported multilayered plate embedded with SMA wires (without pre-strained) under only mechanical loading but in different temperature (isothermal condition) is investigated. In this regard, a plate lamination scheme $[0°/90°/90°/0°]_s$ is considered. It is assumed that the SMA wires with volume fraction of 40% are embedded in the layers 1 and 8 in the x direction and also layers 2 and 7 in the y direction. The material properties of the SMA wires are presented in Table 2. The material and also geometrical properties of the plate are as bellows:

$$E_1 = 50\,\text{GPa}, \quad E_2 = E_3 = 10\,\text{GPa}, \quad G_{12} = G_{13} = G_{23} = 5\,\text{GPa},$$
$$\nu_{12} = \nu_{13} = \nu_{23} = 0.25$$
$$\alpha_L = 1.5e - 8°\text{C}^{-1}, \quad \alpha_T = 1e - 6°\text{C}^{-1}, \quad \rho = 1600\,\text{kg/m}^3$$

A step impulsive pressure with amplitude $P = 3$ MPa P = 4 MPa is applied on the top surface of the plate in the z direction P = 4MPa. Figure 3 shows the response history at the center of the plate. As can be seen in this figures, the vibration amplitude decreases gradually. The reason of this phenomenon is the phase transformation in the SMA wires.

Loss factor of the SMA multilayered plate is evaluated using the measurement of the vibration amplitude within the vibration and the below relation:

$$\zeta = \frac{1}{2\pi}\frac{1}{n}\ln\left(\frac{x_1 - x_{mean}}{x_{n-1} - x_{mean}}\right) \tag{71}$$

According to Figure 3 it can be seen that as the temperature increases, the SMA wires exhibit lower capability in damping the response amplitude such that the loss factors of the response are 1/59%, 1/44%, 1/05%, 0/65% and 0/38% for temperatures 50°C, 55°C, 60°C, 65°C and 70°C, respectively. In other words, the hysteresis level is decreased with increasing the temperature. The reason is that the critical stress for the start of the phase transformation increased with increasing the temperature and therefore the less phase transformation is occurred in the SMA wires. In the next part, a transient nonlinear dynamic analysis of simply supported multilayered plate embedded with pre-strained SMA wires considering both shape memory and pseudoelastic effects, under mixed thermal- mechanical loading investigated. For this aim the SMA wires are pre-strained up to 0.5% at low temperature 20 °Cand embedded in the layers. Further, the SMA hybrid composite plate is heated up to = 50°C, meanwhile the plate undergoes the impulse mechanical loading. The deflection response at the center of the plate is shown in Figure 4. In this figure two cases are studied. In the first case the pre-strained is zero (e = 0) and in the second case the pre-strained is 0.5% (e = 0.5%).

According to Figure 3 it can be seen that when the pre-strain of SMA wires is considered, a remarkable reduction in the amplitude of response occurred such that the amplitude of the first pick reduced more than 10%. The reason of this phenomenon is that upon the thermal condition, due to the shape memory effect of pre-strained SMA wires, the recovery stress (see Figure 4) is generated in the SMA wires and therefore increases the stiffness of the structure. The recovery stress for the center of the top layer is marked with point A in the Figure 4. Also a history of martesite volume fraction for the center of the top layer is shown in Figure 5. Interpretation of the recovery stress is described as: It is assumed that the SMA

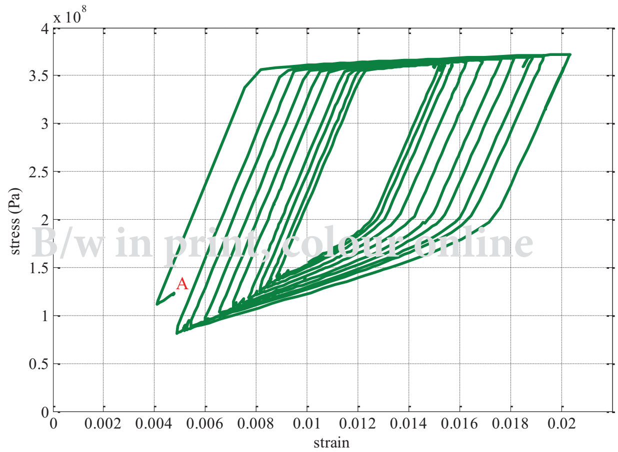

Figure 4. Stress-strain curve for the center of the top layer of the plate for thermal-mechanical loading.

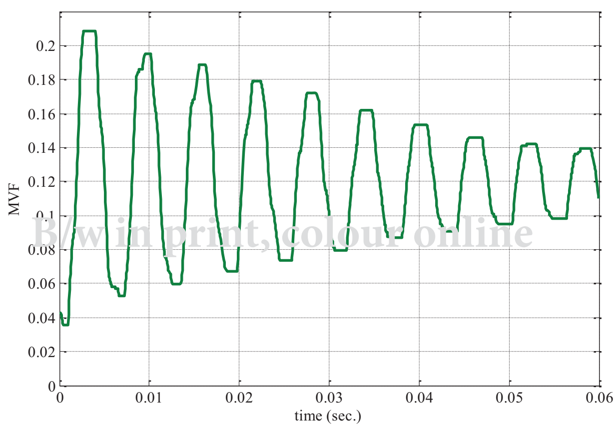

Figure 5. Variation of martesite volume fraction with time for the center of the top layer of the plate for thermal-mechanical loading.

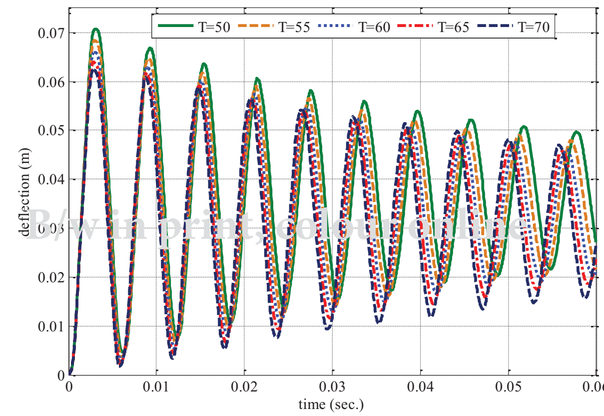

Figure 7. Response history of deflection at the center of the plate for different thermal loading and e0 = 0.5%.

wire is pre-strained at the low temperature (less than M_f). When the ends of SMA wire are free, upon the thermal loading, the SMA wires tend to come back to its original shape (line $A_s \rightarrow A_f$ in Figure 6) or pre-strained is removed (this characteristic of SMA is called shape memory effect). But when the ends of SMA wire are constrained, upon the thermal loading, the SMA wires tend to come back to its original shape, but the constraints prevent from this coming back and therefore according to line $A_s \rightarrow A_1$ in Figure 6, the recovery stress is generated in the SMA wires.

The recovery stresses obtained from this research are compared with results reported by Rezaei et al. in ref. [24]. As can be seen a good agreement is obtained.

Figure 7 shows the response of the plate for different thermal loading with pre-strained e0 = 0.5%. It can be seen that as the temperature increases, due to the increasing of the recovery stresses, the reduction of vibrational amplitude increases, especially for the first amplitude. It must be mentioned that, as can be seen from Figure 7, the reduction of amplitude for the last cycles of response is not remarkable. The reason is that, as mentioned in the case of isothermal condition (see Figure 3) with increasing the temperature the loss factor of the response decreased.

Figure 8 shows the response of the plate for different pre-strained of the SMA wires and specified thermal loading up to T = 50. It can be seen that as the pre-strained increases, due to the increasing of the recovery stresses, the reduction of vibrational amplitude increases. One important point from this figure is that in contrast with many studies reported before, it cannot be always say that the reduction of deflection's amplitude is increased with increasing the pre-strain of SMA wires. Because as can be seen in Figure 8, for a specified increasing in temperature, with increasing the pre-strain, only a limit reduction of deflection's amplitude can be obtained. The reason is that, as can be seen in Figure 11, for a specified increasing in

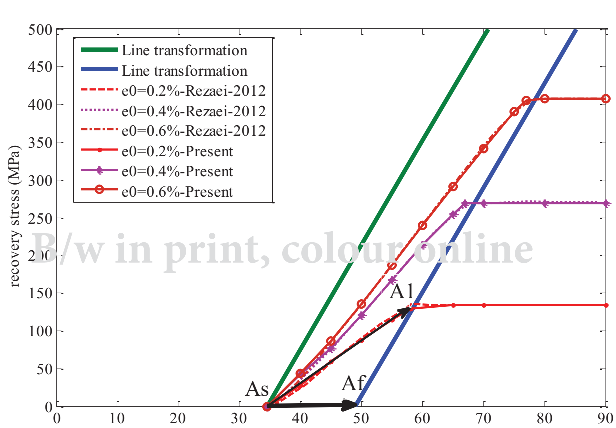

Figure 6. Diagram of martensite-stress-temperature and recovery stress for different pre-strained.

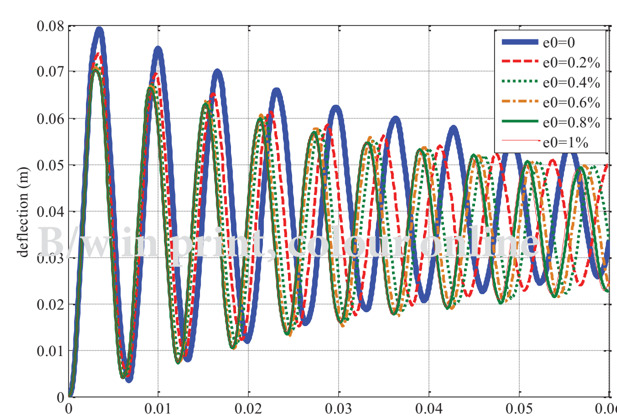

Figure 8. Response history of deflection at the center of the plate for different pre-strain and thermal loading to T = 50.

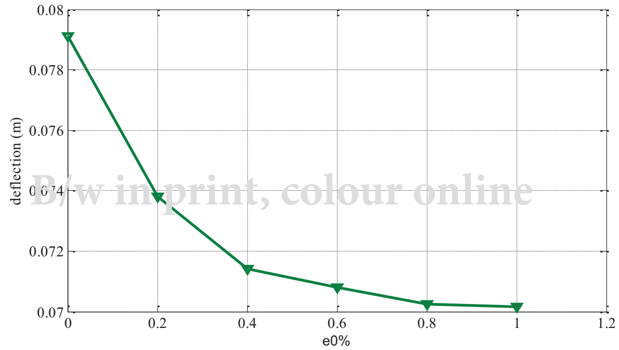

Figure 9. The amplitude of the first pick of the response for different pre-strain and thermal loading to T = 50.

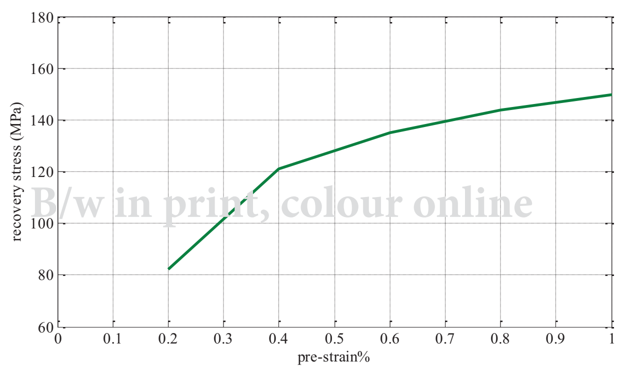

Figure 10. The recovery stress for different pre-strain and thermal loading up to T = 50.

temperature, with increasing the pre-strain of the SMA wires the recovery stress converges to the constant value. In other words, for obtaining a more recovery stress induced by increasing the pre-strain, more thermal loading is needed. For example according to Figure 11 it can be seen that, in order to generating the more recovery stress in the SMA wires with pre-strain 0.2%, 0.4% and 0.6%, the temperature must be increased up to A_1, A_2 and A_3 respectively.

It is well known that the boundary conditions have an important effect on the response of the plate. For this aim, the boundary conditions SSSS, CCCC and CSCS are investigated, where S

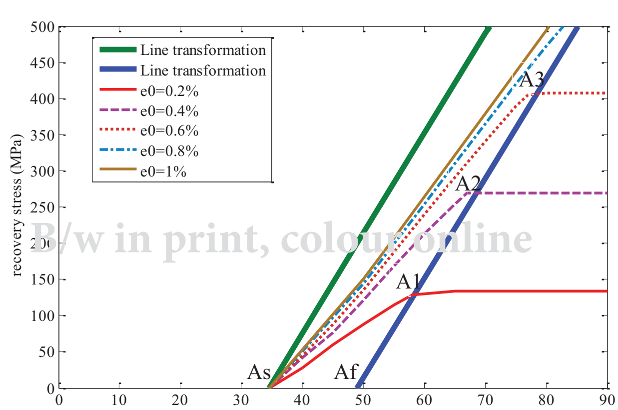

Figure 11. Diagram of martensite-stress-temperature and recovery stress for pre-strained less than 1%.

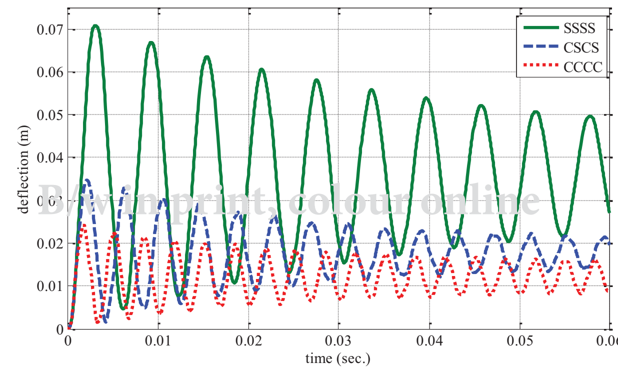

Figure 12. Response history of deflection at the center of the plate with e0 = 0.5% and thermal loading up to T = 50.

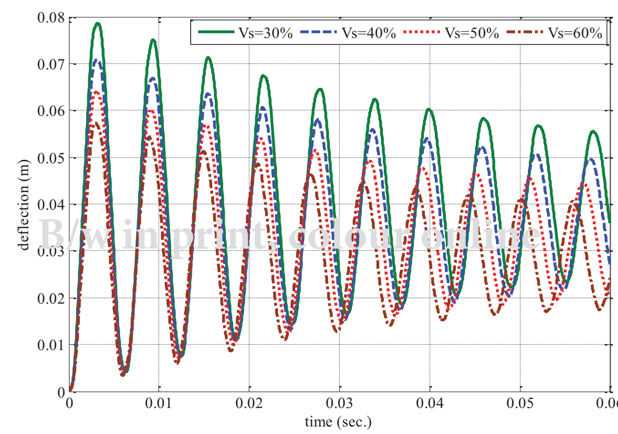

Figure 13. Response history of deflection at the center of the plate for different volume fraction of SMA wires, with e0 = 0.5% and thermal loading up to T = 50.

and C mean the simply supported and clamped boundary conditions, respectively. The results are shown in Figure 12 for pre-strained e0 = 0.5% and thermal loading up to T = 50.

The effect of volume fraction of SMA wires on the response of the plate with pre-strain of SMA wires e0 = 0.5% and thermal loading up to 50 is studied in Figure 13. It can be seen that, with increasing the volume fraction of the SMA wires, the reduction of the deflection's amplitude is very remarkable.

The distribution of recovery stresses along the top layer of the plate is shown in Figure 13. One important point is that in many researches, it is assumed that the recovery stresses is constant along the plate. While as can be seen in the Figure 14, the recovery stress is variable for different points along the plate.

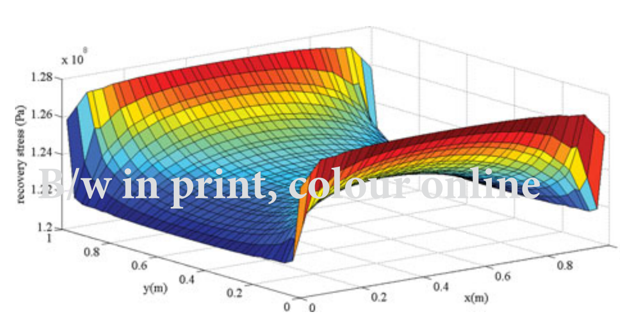

Figure 14. Distribution of recovery stresses along the top layer of the plate, with e0 = 0.5% and thermal loading up to T = 50.

6. Conclusion

In this research, a nonlinear dynamic analysis of multilayered composite plate embedded with pre-strained SMA wires under thermal condition is investigated considering both effects of SMAs simultaneously. The constitutive equation proposed by Brinson is used for modelling the behaviors of SMA wires. The equations of motion are derived in the framework of Carrera's Unified Formulation, based on the RMVT. In this regard, the nonlinear strains are employed for modelling the thermal effects and also the effect of recovery stresses in the SMA wires. The Newmark method is used for the time integration of the equations. For solving the coupled equations, a transient nonlinear finite element in conjunction with incremental iterative algorithm proposed by the author is employed. Results show that upon the thermal condition, the recovery stress is generated in the SMA wires and therefore reduce the amplitude of a damped response of the plate. Several numerical examples upon effect of different thermal condition, different volume fraction of SMA wires and different boundary conditions have been analyzed. Also the effect of the pre-strain of the SMA wires on the response of the plate is extensively investigated for the first time.

Acknowledgments

This research was supported by Shahrekord University, so the author would like to thank the Authorities of Shahrekord University for their great attention.

References

[1] A. Parhi and B. N. Singh, "Nonlinear free vibration analysis of shape memory alloy embedded laminated composite shell panel," *Mechan. Adv. Mat. Struct.*, vol. 24, (9), pp. 713–724, 2017. doi:10.1080/15376494.2016.1196777.

[2] L. Xue, G. Dui, B. Liu and J. Zhang, "Theoretical analysis of a functionally graded shape memory alloy plate under graded temperature loading," *Mech. Adv. Mat. Struct.*, vol. 23, (10), pp. 1181–1187, 2016. doi:10.1080/15376494.2015.1068398.

[3] S. M. R. Khalili, M. Botshekanan Dehkordi and E. Carrera, "A nonlinear finite element model using a unified formulation for dynamic analysis of multilayer composite plate embedded with SMA wires," *Comp. Struct.*, vol. 106, pp. 635–645, 2013. doi:10.1016/j.compstruct.2013.07.006.

[4] M. Botshekanan, S. M. R. Dehkordi and E. Khalili, Carrera, "Nonlinear transient dynamic analysis of sandwich plate with composite face-sheets embedded with shape memory alloy wires and flexible core- based on the mixed LW (layer-wise)/ESL (equivalent single layer) models", *Comp. Part B: Eng.*, vol. 87, pp. 59–74, 2016. doi:10.1016/j.compositesb.2015.10.008.

[5] M. Botshekanan Dehkordia and S. M. R. Khalili, "Frequency analysis of sandwich plate with active SMA hybrid composite face-sheetstemperature dependent flexible core," *Comp. Struct.*, vol. 123, pp. 408–419, 2015. doi:10.1016/j.compstruct.2014.12.068.

[6] A. Eshghinejad and M. Elahinia, "Exact solution for bending of shape memory alloy beams," *Mech. Adv. Mat Struct.*, vol. 22, (10), pp. 829–838, 2015. doi:10.1080/15376494.2013.864435.

[7] L. C. Shiaua, S. Y. Kuob and S. Y. Changa, "Free vibration of buckled SMA reinforced composite laminates," *Comp. Struct.*, vol. 93, (11), pp. 2678–2684, 2011. doi:10.1016/j.compstruct.2011.06.008.

[8] M. Z. Kabir and B. Tavousi Tehrani, "Closed-form solution for thermal, mechanical, and thermo-mechanical buckling and post-buckling of SMA composite plates," *Comp Struct.*, vol. 168, pp. 535–548, 2017. doi:10.1016/j.compstruct.2017.02.046.

[9] S. M. R. Khalilia and A. Ardaliab, "Low-velocity impact response of doubly curved symmetric cross-ply laminated panel with embedded SMA wires," *Comp. Struct.*, vol. 105, pp. 216–226, 2013. doi:10.1016/j.compstruct.2013.04.041.

[10] H. Asadi, M. Bodaghi, M. Shakeri and M. M. Aghdam, "An analytical approach for nonlinear vibration and thermal stability of shape memory alloy hybrid laminated composite beams," *Eur J MechA/Sol.*, vol. 42, pp. 454–468, 2013. doi:10.1016/j.euromechsol.2013.07.011.

[11] H. Asadi, A. H. Akbarzadeh and Q. Wang, "Nonlinear thermo-inertial instability of functionally graded shape memory alloy sandwich plates," *Comp. Struct.*, vol. 120, pp. 496–508, 2015. doi:10.1016/j.compstruct.2014.10.027.

[12] V. Birman, K. Chandrashekhara and S. Sain, "An approach to optimization of shape memory alloy hybrid composite plates subjected to low-velocity impact," *Compos Part B Eng.*, vol. 27B, pp. 439–46, 1996. doi:10.1016/1359-8368(96)00010-8.

[13] G. Kirchhoff, "Uber das Cleichwich und die Bewegung einer Elastischen Sheibe," *J Reine Angew Math.*, vol. 40, pp. 51–88, 1950.

[14] E. Reissner, "The effects of transverse shear deformation on the bending of elastic plates," *J Appl Mech.*, vol. 12, pp. 69–76, 1945.

[15] R. D. Mindlin, "Influence of rotatory inertia and shear on flexural motions of isotropic elastic plates," *J Appl Mech.*, vol. 18, pp. 1031–6, 1951.

[16] S. Srinivas and A. X. Rao, "Bending, vibration and buckling of simply supported thick orthotropic rectangular plates and laminates," *Int J Solid Struct.*, vol. 6, pp. 1463–81, 1970. doi:10.1016/0020-7683(70)90076-4.

[17] E. Carrera, "A class of two-dimensional theories for anisotropic multilayered plates analysis," *Atti Accad Sci Torino Mem Sci Fis.*, vol. 19–20, pp. 1–39, 1995.

[18] E. Carrera and L. Demasi, "Multilayered finite plate element based on Reissner's mixed variational theorem," *Part I: Theory. Int J Numer Methods Eng.*, vol. 55, pp. 191–231, 2002.

[19] E. Carrera and L. Demasi, "Multilayered finite plate element based on Reissner's mixed variational theorem," *Part I: Numerical analysis. Int J Numer Methods Eng.*, vol. 55, pp. 253–91, 2002.

[20] E. Carrera, "Theories and finite elements for multilayered plates and shells: a unified compact formulation with numerical assessment and benchmarking," *Arch Comput Methods Eng.*, vol. 10, pp. 215–96, 2003. doi:10.1007/BF02736224.

[21] L. C. Brinson and R. Lammering, "Finite element analysis of the behavior of shape memory alloys and their applications," *Int J Solids Struct.*, vol. 30, (23):3261–3280, 1993. doi:10.1016/0020-7683(93)90113-L.

[22] J. N. Reddy, *An Introduction to Nonlinear Finite Element Analysis*. Oxford university press, New York, 2004.

[23] A. J. Zak, M. P. Cratmell and W. Ostachowicz, "Dynamics of multilayered composite plates with shape memory alloy wires," *J Appl Mech.*, vol. 70, pp. 313–27, 2003. doi:10.1115/1.1546263.

[24] S. H. Rezaei DA, M. Kadkhodaei and H. Nahvi; "Analysis of nonlinear free vibration and damping of a clamped-clamped beam with embedded prestrained shape memory alloy wires"; *J. Int Mat Sys Struct.*, vol. 23(10): 1107–1117; 2012. doi:10.1177/1045389X12441509.

Apendix

$$
\begin{aligned}
K_{uuxx}^{k\tau sij}(\xi) = {} & \triangleleft \tilde{Z}_{pp11}^{k\tau s}(\xi)[N_{i,x}N_{j,x}]\triangleright_\Omega + \triangleleft \tilde{Z}_{pp16}^{k\tau s}(\xi)[N_{i,y}N_{j,x}]\triangleright_\Omega \\
& + \triangleleft \tilde{Z}_{pp16}^{k\tau s}(\xi)[N_{i,x}N_{j,y}]\triangleright_\Omega \\
& + \triangleleft \tilde{Z}_{pp66}^{k\tau s}(\xi)[N_{i,y}N_{j,y}]\triangleright_\Omega \\
K_{uuxy}^{k\tau sij}(\xi) = {} & \triangleleft \tilde{Z}_{pp12}^{k\tau s}(\xi)[N_{i,x}N_{j,y}]\triangleright_\Omega + \triangleleft \tilde{Z}_{pp26}^{k\tau s}(\xi)[N_{i,y}N_{j,y}]\triangleright_\Omega \\
& + \triangleleft \tilde{Z}_{pp16}^{k\tau s}(\xi)[N_{i,x}N_{j,x}]\triangleright_\Omega \\
& + \triangleleft \tilde{Z}_{pp66}^{k\tau s}(\xi)[N_{i,y}N_{j,x}]\triangleright_\Omega
\end{aligned}
$$

$$K_{uuxz}^{k\tau sij}(\xi) = 0$$

$$K_{uuyx}^{k\tau sij}(\xi) = \lhd \tilde{Z}_{pp12}^{k\tau s}(\xi)[N_{i,y}N_{j,x}]\rhd_\Omega + \lhd \tilde{Z}_{pp16}^{k\tau s}(\xi)[N_{i,x}N_{j,x}]\rhd_\Omega + \lhd \tilde{Z}_{pp26}^{k\tau s}(\xi)[N_{i,y}N_{j,y}]\rhd_\Omega + \lhd \tilde{Z}_{pp66}^{k\tau s}(\xi)[N_{i,x}N_{j,y}]\rhd_\Omega$$

$$K_{uuyy}^{k\tau sij}(\xi) = \lhd \tilde{Z}_{pp22}^{k\tau s}(\xi)[N_{i,y}N_{j,y}]\rhd_\Omega + \lhd \tilde{Z}_{pp26}^{k\tau s}(\xi)[N_{i,x}N_{j,y}]\rhd_\Omega + \lhd \tilde{Z}_{pp26}^{k\tau s}(\xi)[N_{i,y}N_{j,x}]\rhd_\Omega + \lhd \tilde{Z}_{pp66}^{k\tau s}(\xi)[N_{i,x}N_{j,x}]\rhd_\Omega$$

$$K_{uuyz}^{k\tau sij}(\xi) = 0$$

$$K_{uuzx}^{k\tau sij}(\xi) = 0$$

$$K_{uuzy}^{k\tau sij}(\xi) = 0$$

$$K_{uuzz}^{k\tau sij}(\xi) = 0$$

$$K_{u\sigma xx}^{k\tau sij}(\xi) = E_{\tau_{,z}s}\lhd[N_iN_j]\rhd_\Omega$$

$$K_{u\sigma xy}^{k\tau sij}(\xi) = 0$$

$$K_{u\sigma xz}^{k\tau sij}(\xi) = \lhd \tilde{Z}_{pn13}^{k\tau s}(\xi)[N_{i,x}N_j]\rhd_\Omega + \lhd \tilde{Z}_{pn36}^{k\tau s}(\xi)[N_{i,y}N_j]\rhd_\Omega$$

$$K_{u\sigma yx}^{k\tau sij}(\xi) = 0$$

$$K_{u\sigma yy}^{k\tau sij}(\xi) = E_{\tau_{,z}s}\lhd[N_iN_j]\rhd_\Omega$$

$$K_{u\sigma yz}^{k\tau sij}(\xi) = \lhd \tilde{Z}_{pn23}^{k\tau s}(\xi)[N_{i,y}N_j]\rhd_\Omega + \lhd \tilde{Z}_{pn36}^{k\tau s}(\xi)[N_{i,x}N_j]\rhd_\Omega$$

$$K_{u\sigma zx}^{k\tau sij}(\xi) = E_{\tau s}\lhd[N_{i,x}N_j]\rhd_\Omega$$

$$K_{u\sigma zy}^{k\tau sij}(\xi) = E_{\tau s}\lhd[N_{i,y}N_j]\rhd_\Omega$$

$$K_{u\sigma zz}^{k\tau sij}(\xi) = E_{\tau_{,z}s}\lhd[N_iN_j]\rhd_\Omega$$

$$K_{\sigma uxx}^{k\tau sij}(\xi) = E_{\tau s_{,z}}\lhd[N_iN_j]\rhd_\Omega$$

$$K_{\sigma uxy}^{k\tau sij}(\xi) = 0$$

$$K_{\sigma uxz}^{k\tau sij}(\xi) = E_{\tau s_{,z}}\lhd[N_iN_j]\rhd_\Omega$$

$$K_{\sigma uyx}^{k\tau sij}(\xi) = 0$$

$$K_{\sigma uyy}^{k\tau sij}(\xi) = E_{\tau s_{,z}}\lhd[N_iN_j]\rhd_\Omega$$

$$K_{\sigma uyz}^{k\tau sij}(\xi) = E_{\tau s}\lhd[N_iN_{j,y}]\rhd_\Omega$$

$$K_{\sigma uzx}^{k\tau sij}(\xi) = -\lhd \tilde{Z}_{np13}^{k\tau s}(\xi)[N_iN_{j,x}]\rhd_\Omega - \lhd \tilde{Z}_{np36}^{k\tau s}(\xi)[N_iN_{j,y}]\rhd_\Omega$$

$$K_{\sigma uzy}^{k\tau sij}(\xi) = -\lhd \tilde{Z}_{np23}^{k\tau s}(\xi)[N_iN_{j,y}]\rhd_\Omega - \lhd \tilde{Z}_{np36}^{k\tau s}(\xi)[N_iN_{j,x}]\rhd_\Omega$$

$$K_{\sigma uzz}^{k\tau sij}(\xi) = E_{\tau s_{,z}}\lhd[N_iN_j]\rhd_\Omega$$

$$K_{\sigma\sigma xx}^{k\tau sij}(\xi) = -\lhd \tilde{Z}_{nn55}^{k\tau s}(\xi)[N_iN_j]\rhd_\Omega$$

$$K_{\sigma\sigma xy}^{k\tau sij}(\xi) = -\lhd \tilde{Z}_{nn45}^{k\tau s}(\xi)[N_iN_j]\rhd_\Omega$$

$$K_{\sigma\sigma xz}^{k\tau sij}(\xi) = 0$$

$$K_{\sigma\sigma yx}^{k\tau sij}(\xi) = -\lhd \tilde{Z}_{nn45}^{k\tau s}(\xi)[N_iN_j]\rhd_\Omega$$

$$K_{\sigma\sigma yy}^{k\tau sij}(\xi) = -\lhd \tilde{Z}_{nn44}^{k\tau s}(\xi)[N_iN_j]\rhd_\Omega$$

$$K_{\sigma\sigma yz}^{k\tau sij}(\xi) = 0$$

$$K_{\sigma\sigma zx}^{k\tau sij}(\xi) = 0$$

$$K_{\sigma\sigma zy}^{k\tau sij}(\xi) = 0$$

$$K_{\sigma\sigma zz}^{k\tau sij}(\xi) = -\lhd \tilde{Z}_{nn33}^{k\tau s}(\xi)[N_iN_j]\rhd_\Omega$$